CERN - EUROPEAN ORGANIZATION FOR NUCLEAR RESEARCH

Submitted to
Nuclear Physics B.

CERN/EP/PHYS 77-47
20 September 1977

TOTAL CROSS SECTIONS FOR ν_e AND $\bar{\nu}_e$ INTERACTIONS AND SEARCH FOR NEUTRINO OSCILLATIONS AND DECAY

Gargamelle Collaboration

J. BLIETSCHAU, H. DEDEN, F.J. HASERT, W. KRENZ, D. LANSKE, J. MORFIN, M. POHL, K. SCHULTZE, H. SCHUMACHER, H. WEERTS and L.C. WELCH
III. Physikalisches Institut der Technischen Hochschule, Aachen, Germany.

G. BERTRAND-COREMANS, M. DEWIT(*), H. MULKENS(**), J. SACTON and W. VAN DONINCK(***)
Interuniversity Institute for High Energies, U.L.B., V.U.B. Brussels, Belgium.

D. HAIDT, C. MATTEUZZI, P. MUSSET, B. PATTISON, F. ROMANO(+), J.P. VIALLE(++) and A. WACHSMUTH
CERN, European Organization for Nuclear Research, Geneva, Switzerland.

A. BLONDEL, V. BRISSON, B. DEGRANGE, T. FRANÇOIS, M. HAGUENAUER, U. NGUYEN-KHAC and P. PETIAU
Laboratoire de Phys. Nucl. des Hautes Energies, Ecole Polytechnique, Paris, France.

E. BELLOTTI, S. BONETTI, D. CAVALLI, E. FIORINI, A. PULLIA and M. ROLLIER
Istituto di Fisica dell'Università and INFN, Milano, Italy.

B. AUBERT, D. BLUM, A.M. LUTZ and C. PASCAUD
Laboratoire de l'Accélérateur Linéaire, Orsay, France.

F.W. BULLOCK and A.G. MICHETTE(+++)
University College London, London, U.K.

(*) Fellowship IRSIA.

(**) Chercheur agréé de l'IISN, Belgium.

(***) Vorser, IIKW, Belgie.

(+) Now at University of Bari, Italy.

(++) On leave of absence from the LAL, Orsay, France.

(+++) Now at Rutherford Laboratory, Chilton, Didcot, U.K.

EF/ef

CERN/EP/PHYS 77-47

ABSTRACT

About 200 and 60 candidates for electron neutrino and antineutrino interactions, respectively, have been analyzed in the heavy liquid bubble chamber Gargamelle exposed to the CERN PS neutrino beam. Evidence for scaling has been found for these interactions, with slopes of the cross sections in good agreement with those obtained for muon neutrino and antineutrino events in the same chamber. No evidence appears for oscillations of neutrinos or antineutrinos, which would induce in the present experiment an excess of electron or positron events. The corresponding limits are given as functions of the mixing parameter, for the finite mass Majorana neutrinos. The possibility of a multiplicative law for the lepton number has also been investigated. A search for isolated electron-positron pairs revealed no excess in the forward direction, in contradiction to the expectation for muonic neutrino and antineutrino decays. The corresponding limits on the centre of mass half lifetimes are given.

1. INTRODUCTION

Although extensive studies of the interactions of muonic neutrinos in the range 0.5 to 200 GeV have been performed in the last few years, very little is known about the electronic neutrino interactions in this energy range. In 1973, the Gargamelle Collaboration [1] reported first results on the two processes

$$\nu_e + N \to e^- + \text{hadrons} \quad (45 \text{ events}) \tag{1}$$

$$\bar{\nu}_e + N \to e^+ + \text{hadrons} \quad (7 \text{ events}) \tag{2}$$

using the ν_e, $\bar{\nu}_e$ contamination present in the CERN PS ν_μ and $\bar{\nu}_\mu$ beams.

Since that time, much larger statistics have been accumulated in Gargamelle and the present work is based on the analysis of about 200 electron and 60 positron events allowing a better study of the above processes. The old data are not included in this analysis.

The present sample has also been used to investigate the possible existence of $\nu_\mu \rightleftarrows \nu_e$ oscillations and of the lepton multiplicative law. In addition, in the course of a search for the elastic processes $\nu_\mu(\bar{\nu}_\mu) + e^- \to \nu_\mu(\bar{\nu}_\mu) + e^-$, a scan has been performed for all isolated e^+e^- pairs in the visible volume of the chamber [2,3]. This information is analyzed in view of setting a limit on the neutrino lifetime from its hypothetical electromagnetic decay

$$\nu(\bar{\nu}) \to \gamma + \nu'(\bar{\nu}') \ . \tag{3}$$

2. EXPERIMENTAL PROCEDURE

2.1 The beam

During the CERN neutrino (antineutrino) experiments the muon radial flux was continuously monitored at different depths in the steel shielding. In a separate experiment, the K to π production ratio was measured using 24 GeV protons [4] on a Be target i.e., in conditions similar to the ones realized when running the $\nu(\bar{\nu})$ experiments. Combining this information, the $\nu_\mu(\bar{\nu}_\mu)$ flux and energy spectrum can be determined. The $\nu_e(\bar{\nu}_e)$

contaminations present in the $\nu_\mu(\bar{\nu}_\mu)$ beams are then calculated on the basis of the additive lepton conservation law, and found to be at the level of a few tenths of a percent below about 3 GeV and to rise to 2 or 3% at higher energies (fig. 1). Below 2 or 3 GeV, the dominant source of ν_e and $\bar{\nu}_e$ is muon decay, while above that limit most of the ν_e and $\bar{\nu}_e$ come from the electronic decay modes of charged kaons and to a lesser extent from K^o_L mesons. Then, latter also leads to $\bar{\nu}_e(\nu_e)$ contaminations in the $\nu_\mu(\bar{\nu}_\mu)$ beams. The relative contributions of the various $\nu_e(\bar{\nu}_e)$ sources are illustrated in fig. 1. It should be noted that the ν_e spectrum in the ν_μ beam is "harder" than the $\bar{\nu}_e$ spectrum in the $\bar{\nu}_\mu$ beam as a consequence of a higher K to π production ratio for positive secondaries. Also, the ν_e contamination in the $\bar{\nu}_\mu$ beam is significantly higher than the $\bar{\nu}_e$ content in the ν_μ beam.

2.2 The detector

The heavy liquid bubble chamber Gargamelle was filled with heavy freon CF_3Br. The short radiation length (X_o = 11 cm) of the liquid ensures an excellent identification of the electrons and the positrons through the observation of bremsstrahlung and track spiralization. The fiducial volume ($\sim$ 3 m^3) was chosen to provide a mean potential path length of about 150 cm for the particles produced in the $\nu(\bar{\nu})$ interactions, allowing a reliable separation of the muons from the hadrons (hadron interaction length of about 60 cm).

2.3 Scanning measurements and event selection

The $\nu_e(\bar{\nu}_e)$ induced reactions are signed by the presence of an electron (positron) among the secondary products. For the present study, 192 000 pictures taken in the ν_μ beam and 998 000 pictures in the $\bar{\nu}_\mu$ beam were analyzed; these statistics correspond to respectively 1.1×10^{18} and 4.5×10^{18} protons on the target or to 4.4×10^{15} ν's and 1×10^{16} $\bar{\nu}$'s traversing the fiducial volume of Gargamelle. The $\bar{\nu}$ pictures were double scanned for all antineutrino and neutrino charged and neutral current induced reactions. The ν pictures were selectively double scanned for events

containing electrons of either charge and/or e^+e^- pairs whose vertices are close or attached to the neutrino interaction point. In both cases, all isolated electrons, positrons and e^+e^- pairs were recorded.

All events inside the 3 m^3 fiducial volume were carefully checked. Only those electrons and positrons attached to the vertex, showing at least one materialized bremsstrahlung γ-ray and having an energy greater than 200 MeV were retained for the analysis. To avoid confusion with Dalitz pairs and electron pairs materialized in spatial coincidence with the neutrino interaction point, it was required that the electron (positron) appears clearly as a single track over a distance in space of 2.5 cm before shower development. The loss of genuine electrons (positrons) resulting from the application of this procedure was estimated, as a function of the electron energy, by a Monte-Carlo calculation simulating electrons and positrons in the chamber. The electron identification efficiency W is reported in table I, as a function of the electron energy.

Due to the short radiation length of the liquid, the curvature of the electron track in the Gargamelle magnetic field cannot always be measured before shower development. The fraction of the events for which the sign of the electron charge remains, thus, ambiguous was found to be 25% and 35% in the $\bar{\nu}$ and ν films, respectively. Most of these electrons have an energy greater than 1.5 GeV However, this sign ambiguity could be resolved in many cases by estimating for each event the azimuthal asymmetry induced by the magnetic field in the development of the electromagnetic shower, with respect to the direction of emission of the electron. The remaining $e^\pm$ events (about 10% of the events in both films) have then been distributed in the e^+ and e^- categories according to the relative population of these categories as a function of the electron energy.

The scanning efficiencies for $\nu_e(\bar{\nu}_e)$ events and isolated $e^\pm$ or e^+e^- pairs were found to be 97% and 92% respectively.

The energy of the neutrino (antineutrino) event is taken to be the total visible energy liberated in the interaction, corrected for the energy taken off by undetected neutrons and γ rays from π^o decays and unmeasurable

tracks. Further details about the procedure can be found in refs [5,6]. The neutrino energy is determined with an average uncertainty of about 25%, almost entirely due to the 30% error affecting the electron energy.

Only those events with total energy $E_{\nu,\bar{\nu}} > 1$ GeV and longitudinal momentum along the beam axis, $P_L > 0.6$ GeV/c were retained for the present analysis, as in the case of muon neutrinos [5].

3. RESULTS

3.1 Inclusive ν_e and $\bar{\nu}_e$ interactions

The number of events containing an electron or a positron of energy greater than 200 MeV corrected for electron detection efficiency (table 1) are listed in table 2 as a function of the neutrino (antineutrino) energy. It is to be noted that 80% of the e^+ events observed in the ν film contain an additional μ^- candidate, whilst this fraction is only of about 20% for the e^- events. It was shown in a previous paper that the bulk of these $e^+\mu^-$ events are indeed ν_μ induced events [7]. Therefore, the following analysis of ν_e and $\bar{\nu}_e$ interactions will be based respectively on the e^- events from both ν and $\bar{\nu}$ films and on the e^+ events from the $\bar{\nu}$ films only.

In these three samples, the background due to both ν_μ and $\bar{\nu}_\mu$ charged and neutral current events in which an asymmetric e^+e^- pair attached to the interaction vertex simulates an electron or a positron has been estimated as a function of the neutrino (antineutrino) energy. This has been done by using empirical estimates of the e^+e^- pair attachment probability ($P_{att} = 4.0 \pm 0.6\%$), the γ asymmetry probabilities ($\alpha^+ = 1.5 \pm 0.4\%$ and $\alpha^- = 4.4 \pm 0.6\%$)(*) as well as the known energy dependence of the γ multiplicities in both ν_μ and $\bar{\nu}_\mu$ charged and neutral current events [7]. The results are displayed in table 2.

As a check of this procedure, the background due to ν_μ and $\bar{\nu}_\mu$ charged current events has been estimated in an independent way. For all $\nu_e(\bar{\nu}_e)$ candidates with all hadrons identified as such, the probability for each hadron to leave the chamber without interacting, and thus, to simulate a μ

(*) α^- also includes the probability for Compton production.

candidate has been calculated taking into account its energy and direction of emission and the measured cross sections for negative and positive hadrons in freon [8]. Within the statistical errors, the results of both methods were found to be in excellent agreement.

Using the ν_e fluxes in both ν and $\bar{\nu}$ beams and the $\bar{\nu}_e$ flux in the $\bar{\nu}$ beam, the total interaction cross sections for ν_e and $\bar{\nu}_e$ have been determined as a function of the neutrino energy from the corrected numbers of events (fig. 2). Account has been taken of the scanning efficiency, of the e-γ confusion probability, of the uncertainty in neutrino fluxes and of the large experimental errors affecting the determination of the neutrino energy. A linear increase of the cross section with energy is observed in both cases, as expected from the scaling hypothesis. The best one-parameter linear fits to these data are

$$\text{for neutrinos:} \qquad (0.7 \pm 0.2)\ E_\nu \times 10^{-38}\ \text{cm}^2/\text{nucleon} \qquad (4)$$

$$\text{for antineutrinos:} \qquad (0.25 \pm 0.07)\ E_{\bar{\nu}} \times 10^{-38}\ \text{cm}^2/\text{nucleon} \qquad (5)$$

and the ratio of the slopes for $\bar{\nu}_e$ and ν_e cross sections is 0.36 ± 0.14.

Scaling also implies a linear rise of the mean value of q^2, the four-momentum transfer squared, with the neutrino energy. This prediction is seen in fig. 3 to be verified within the limits of the available statistics. The best linear fits are

$$\text{for neutrinos:} \qquad (0.18 \pm 0.04)\ E_\nu + (0.1 \pm 0.1) \qquad (6)$$

$$\text{for antineutrinos:} \qquad (0.14 \pm 0.05)\ E_{\bar{\nu}} + (-0.02 \pm 0.10). \qquad (7)$$

As seen from figs 2 and 3, the present data on ν_e and $\bar{\nu}_e$ interactions agree well with the results obtained in similar experimental conditions for ν_μ and $\bar{\nu}_\mu$ [5], as expected from μ-e universality. The ratios of ν_e to ν_μ and $\bar{\nu}_e$ to $\bar{\nu}_\mu$ for the slopes of the cross sections are

$$\sigma_{\nu_e}/\sigma_{\nu_\mu} = 0.95 \pm 0.30 \qquad \sigma_{\bar{\nu}_e}/\sigma_{\bar{\nu}_\mu} = 0.89 \pm 0.30 \qquad (8)$$

in good agreement with μ-e universality. Fig. 4 illustrates the differential cross sections for ν_e and $\bar{\nu}_e$ with respect to the scaling variables $y = \nu/E_{\nu,\bar{\nu}}$, where $\nu = E_\nu(E_{\bar{\nu}}) - E_e(E_e)$ is the energy transfer

from the neutrino to the nucleon in the rest frame of the nucleon target. The curves which interpolate the ν_μ and $\bar{\nu}_\mu$ [9] results are reported for comparison. Here again agreement is seen to exist between both sets of data.

Some examples of V^o particle production have been observed in the ν_e interactions. Among seven candidates, four are identified as $\Lambda^o \to \pi^- p$ and one as $K^o_s \to \pi^+\pi^-$ (3C fits and/or identification of the positive decay product), the remaining two events being compatible with neutron interactions. Using these five events, one gets a raw rate for production of an identified and fitted V^o

$$\frac{\nu_e + N \to e^- V^o + \text{anything}}{\nu_e + N \to e^- + \text{anything}} = (3.8 \pm 1.7)\% \quad . \tag{9}$$

The corresponding raw rate for muon neutrinos is [7]

$$\frac{\nu_\mu + N \to \mu^- V^o + \text{anything}}{\nu_\mu + N \to \mu^- + \text{anything}} = (0.65 \pm 0.05)\% \quad . \tag{10}$$

One should note however that the ν_e spectrum is energetically "harder" than that of muon neutrinos. By weighting the ratio in (10) according to the ν_e spectrum, one obtains

$$\left(\frac{\nu_\mu + N \to \mu^- V^o + \text{anything}}{\nu_\mu + N \to \mu^- + \text{anything}}\right)_{\text{corr.}} = (1.0 \pm 0.09)\% \quad . \tag{11}$$

The statistics are too poor to draw conclusions regarding a possible disagreement between (9) and (11). One possible example of "elastic" Λ^o production by $\bar{\nu}_e$ has been detected in the $\bar{\nu}$ film.

3.2 Neutrino oscillations

Due to the good agreement in the distributions of the scaling variables for events induced by electron and muon neutrinos and anti-neutrinos strict muon-electron universality will be assumed in the following.

In particular, it will be assumed that electron-neutrino and antineutrino cross sections scale as a function of energy with the same slopes as for ν_μ and $\bar{\nu}_\mu$ interactions: $(0.74 \pm 0.08) \times 10^{-38}$ cm^2/GeV, and $(0.28 \pm 0.03) \times 10^{-38}$ cm^2/GeV, respectively [5]. The number of neutrino induced events containing an electron or a positron can then be predicted from the fluxes of neutrinos of different origin in the neutrino beam. The uncertainty in the absolute values of these fluxes has been evaluated to be 30% for neutrino or antineutrino energies between 1 and 2 GeV, and 15% for energies above 2 GeV.

The numbers of predicted events are reported in table 3 separately, for interactions where the electron or positron is associated with an additional lepton candidate (a positive or negative particle which leaves the chamber or decays, or a negative particle which stops), or with "hadronic" tracks only. The "excesses" of the number of events found, corrected for detection efficiency, with respect to those predicted, are also given in this table. The errors include both statistics and uncertainties on the neutrino and antineutrino fluxes and cross sections. The only statistically significant effect, namely the excess of events with a positron in the neutrino film, which is essentially due to events where the positron is associated with a lepton candidate (the muon), can be attributed, as mentioned before, to ν_μ events [7].

As suggested by B. Pontecorvo and by other authors [10-14] violation of the lepton number and the existence of two Majorana neutrinos of finite masses m_1 and m_2 allows the neutrino field to be described in the simplest lepton scheme as

$$\begin{aligned} \nu_e &= \nu_1 \cos\alpha + \nu_2 \sin\alpha \\ \nu_\mu &= -\nu_1 \sin\alpha + \nu_2 \cos\alpha, \end{aligned} \qquad (12)$$

where the angle α is equal to $\pi/4$ for maximum neutrino mixing.

The presence of this mixing would then produce $\nu_\mu \rightleftarrows \nu_e$ and $\bar{\nu}_\mu \rightleftarrows \bar{\nu}_e$ oscillations similar in principle to those of neutral kaons, and an initially "pure" ν_μ beam would contain at a distance R from its origin a ν_e component with intensity

$$\frac{I_{\nu_e}(R,p)}{I^{o}_{\nu_\mu}(R,p)} = 0.5\ (1 - \cos 2\pi \frac{R}{L})\ (\sin^2 2\alpha) \qquad (13)$$

where $I^{o}_{\nu_\mu}(R,p)$ is the muon neutrino intensity in the absence of oscillations and p the neutrino momentum. The oscillation length is given by

$$L = \frac{4\pi p \hbar c}{M^2}, \text{ where } M = \sqrt{|m_1^2 - m_2^2|}\ . \qquad (14)$$

No evidence for oscillation of $\bar{\nu}_e$ has been obtained at a nuclear reactor [15], and in a preceding analysis of published Gargamelle data [16]. In the present experiment, as shown in table 3, no excess is found of electron events (in neutrino pictures) and of positron events (in antineutrino pictures), with respect to those expected from $\nu_e(\bar{\nu}_e)$ component originally present in the beam; the corresponding excesses being $(-0.03 \pm 0.1)\%$ and $(0.02 \pm 0.07)\%$ with respect to the ν_μ and $\bar{\nu}_\mu$ events, respectively. The corresponding limits depend both on the mixing angle and on the mass M in eq. (14). Eq. (13) has been weighted by means of a Monte-Carlo method on the neutrino momentum distribution and on the distribution of neutrino origins inside the decay tunnel. The corresponding limits at 68% and 95% confidence levels on the parameter M for fixed values of the mixing angle are reported in fig. 5 for neutrinos and antineutrinos.

3.3 A limit on the lepton multiplicative law

If the multiplicative law for the muon number is valid [17,18] both decays

$$\mu^+ \to e^+ + \nu_e + \bar{\nu}_\mu \qquad \mu^- \to e^- + \bar{\nu}_e + \nu_\mu \qquad (15)$$

and

$$\mu^+ \to e^+ + \bar{\nu}_e + \nu_\mu \qquad \mu^- \to e^- + \nu_e + \bar{\nu}_\mu \qquad (16)$$

are allowed, while only decays (15) are allowed by the additive law. The multiplicative law predicts therefore that the component of electron neutrino flux from positive and negative muon decay is equally divided in electron neutrino and antineutrinos. This implies an excess of positrons (electrons) in the neutrino (antineutrino) exposure, and a lack of positrons (electrons) in the antineutrino (neutrino) exposure.

This analysis has been limited to the energy region below 3 GeV, where the contribution to the $\nu_e(\bar{\nu}_e)$ flux due to muon decay is dominant (fig. 1). Defining $\underline{r}$ to be the branching ratio of channel (15) ($\underline{r}$ = 1 and $\underline{r}$ = 0.5 for additive and multiplicative laws, respectively), one obtains from the neutrino exposure

$$\underline{r} = 0.9 \pm 0.3 \text{ (excess of } e^+ \text{ events)}$$
$$\underline{r} = 1.0 \pm 0.6 \text{ (lack of } e^- \text{ events)} \qquad (17)$$

and from the antineutrino exposure

$$\underline{r} = 0.8 \pm 0.2 \text{ (excess of } e^- \text{ events)}$$
$$\underline{r} = 1.3 \pm 0.6 \text{ (lack of } e^+ \text{ events)} . \qquad (18)$$

There is therefore no evidence, either in the neutrino or antineutrino exposure, for a violation of the additive in favour of the multiplcative law.

3.4 A limit on neutrino lifetime

As a consequence of a non-zero mass and of a possible muon number non-conservation, the muon neutrino or antineutrino would decay electromagnetically [13,19,20]

$$\nu_\mu(\bar{\nu}_\mu) \rightarrow \gamma + X , \qquad (19)$$

where X is a neutral object with mass lower than m_{ν_μ} (for instance an electron neutrino or antineutrino).

Measurements of the muon neutrino mass, and particularly the recent result obtained at SIN ($m^2_{\nu_\mu} = (0.1 \pm 0.19)$ MeV^2) [21], ensure that in the present experiment $m_{\nu_\mu} \ll E_{\nu_\mu}$. If in addition, it is assumed that $m_X \ll m_{\nu_\mu}$, the γ-ray energy in the laboratory [19] is given by

$$E_\gamma \simeq 0.5 \, (1 + \cos\theta^*) \, E_{\nu_\mu} , \qquad (20)$$

where θ^* is the angle between γ and ν_μ directions in the neutrino centre of mass system.

Under these conditions the number of γ-rays produced by neutrino decay above a "critical energy" E_c (300 MeV in the present experiment) is given by [19]

$$N = \int_{E_c}^{\infty} \varepsilon\,(E_\gamma)\,\frac{dN}{dE_\gamma}\,dE_\gamma\,, \tag{21}$$

where $\varepsilon\,(E_\gamma)$ is the γ-ray detection efficiency. The γ-ray energy spectrum can be expressed as a function of the neutrino flux

$$\frac{dN}{dE_\gamma} = \frac{m_{\nu_\mu} \cdot 0.693 \cdot \ell}{\tau_{\frac{1}{2}}} \int_0^{\infty} \frac{1}{E_\nu^2}\,\frac{d\,\phi_\nu}{d\,E_\nu}\,d\,E_\nu\,, \tag{22}$$

where ℓ is the length of the fiducial volume.

In this experiment, the large number of neutrinos crossing the chamber (corresponding to 1.75 light years for neutrinos and to 4 light years for antineutrinos) and the high γ-ray detection efficiency, which is rather independent of gamma energy, allow to set a meaningful limit on neutrino lifetime. Since at high energies, the angle of emission of the γ-ray with respect to the incident neutrino direction is small, only those e^+e^- pairs with an angle less than 2° with respect to the beam direction have been considered (the measurement accuracy being $\pm\ 1.5^\circ$). Only one such γ-ray with energy greater than 300 MeV was found in the neutrino and one in the antineutrino film, consistent with the background. From comparison with the predictions of (21) and (22), integrated over the neutrino and antineutrino fluxes, the half lifetimes in the neutrino c.m., at 90% confidence level are found to be

$$\tau_{\frac{1}{2}} > 7 \times 10^{-3}\ s\ m_{\nu_\mu}\ \text{(in eV) for muon neutrinos} \tag{23}$$

and $$\tau_{\frac{1}{2}} > 1.2 \times 10^{-2}\ s\ m_{\bar{\nu}_\mu}\ \text{(in eV) for muon antineutrinos.}$$

The combined limit for neutrinos and antineutrinos is

$$\tau_{\frac{1}{2}} > 1.8\ 10^{-2}\ s\ m_\nu\ \text{(in eV)}$$

to be compared with a limit of 1.5×10^{-3} at the same confidence level, recently obtained for muon neutrinos at Argonne National Laboratory [22].

4. CONCLUSIONS

This analysis shows the linear dependence of the cross sections of electron neutrinos and antineutrinos as a function of energy. The scaling parameters, as well as the ratio between antineutrino and neutrino cross sections are in good agreement with those found previously for muon neutrinos and antineutrinos, thus supporting electron-muon universality.

No excess is found of electron and positron events with respect to the numbers expected from ν_e and $\bar{\nu}_e$ contaminations, respectively. The corresponding limits for the parameter $M = \sqrt{|m_1^2 - m_2^2|}$ for $\nu_\mu \not\rightleftarrows \nu_e$ and $\bar{\nu}_\mu \not\rightleftarrows \bar{\nu}_e$ oscillations are about one electronvolt for maximum mixing of the two Majorana neutrinos, with masses m_1 and m_2.

The data are in agreement with the lepton additive law. From the present analysis of isolated electron-positron pairs no evidence for electromagnetic decay of neutrinos or antineutrinos is found. The 90% C.L. limits on the halftimes in the c.m. system are 7×10^{-3} s m_{ν_μ} (in eV) and 1.2×10^{-2} s $m_{\bar{\nu}_\mu}$ (in eV).

Acknowledgements

The authors would like to thank the beam, chamber, accelerator and scanning teams for their cooperative work.

REFERENCES

[1] T. Eichten et al., Phys. Letters 46B (1973) 281.

[2] F.J. Hasert et al., Phys. Rev. Letters 46B (1973) 121.

[3] J. Blietschau et al., Nucl. Physics 114B (1976) 189.

[4] T. Eichten et al., Nucl. Physics B44 (1972) 333.

[5] T. Eichten et al., Phys. Letters 46B (1973) 274. For the present analysis the uncertainty on the neutrino flux has also been taken into account.

[6] A.M. Lutz, Ph. D. Thesis, LAL 1276, Orsay 1975.

[7] H. Deden et al., Phys. Letters 67B (1977) 474.

[8] W. Van Doninck, to be published.

[9] H. Deden et al., Nucl. Phys. 85B (1975) 269.

[10] S.M. Bilenki and B. Pontecorvo, to be published in Physics Reports.

[11] A.K. Mann and H. Primakoff, Phys. Review D15 (1977) 655.

[12] H. Fritzsch and H.P. Minkowski, Phys. Letters 62B (1976) 72.

[13] S. Eliezer and A.R. Swift, Nucl. Physics 105B (1976) 45.

[14] E. Fiorini, A Note on Neutrino Oscillation Experiments at High Energy Accelerators, University of Milano, preprint, 6 October (1976).

[15] F. Reines, Report to the Aachen International Conference on Neutrino Physics Aachen, 8-12 June (1976).

[16] E. Bellotti, D. Cavalli, E. Fiorini and M. Rollier, Letter al Nuovo Cimento 17 (1976) 553.

[17] R.E. Marshak, Riazzudin and C.P. Ryan, Theory of Weak Interactions in Particle Physics, Monographs and Texts in Physics and Astronomy, Vol. 24 (Interscience).

[18] G. Kalbfleish, Nucl. Physics B25 (1970) 197.

[19] V.E. Barnes, Phys. Letters 65B (1976) 1974.

[20] F. Reines, H.W. Sobel and H.S. Gurr, Phys. Rev. Letters 32 (1974) 180.

[21] M. Daum, G.H. Eaton, R. Frosch, J. McCulloch, R.C. Minehart and E. Steiner, Precision Measurement of Muon Momentum in Stopped Pion Decay, SIN Newsletter No. 7, October (1976).

[22] V.E. Barnes et al., Phys. Rev. Letters 38 (1977) 1049.

TABLE CAPTIONS

Table 1 Identification efficiency as a function of the electron energy. For positrons this efficiency is 4% lower.

Table 2 Energy distribution of electron and positron events with $E_e > 200$ MeV. The background of e^+ in ν film, which is mainly due to the production of dilepton events (table III) is not reported.

Table 3 Events in neutrino and antineutrino film.

TABLE 1

E_e (GeV)	W (%)
0.2	95 ± 3
0.5	90 ± 5
1.0	83 ± 7
1.5	82 ± 10
2.0	78 ± 13
2.5	76 ± 15
3.0	75 ± 17
4.0	68 ± 18
5.0	67 ± 20
7.0	66 ± 25
10.0	64 ± 30

TABLE 2

		$E_{\nu,\bar{\nu}}$ (GeV)	1-2	2-3	3-4	4-5	5-6	> 6
ν film	e^-	Number of events	25.3	25.9	34.3	31.9	20.1	45.3
		Background	2.4 ± 0.6	3.9 ± 1.0	3.5 ± 0.9	2.7 ± 0.7	1.2 ± 0.6	5.6 ± 1.2
	e^+	Number of events	3.3	4.9	1.4	7.2	1.2	7.2
$\bar{\nu}$ film	e^-	Number of events	19.9	13.7	6.5	7.2	4.6	9.1
		Background	1.9 ± 0.5	3.1 ± 0.8	2.1 ± 0.5	1.6 ± 0.4	0.3 ± 0.2	0.9 ± 0.3
	e^+	Number of events	22.6	20.2	11.9	9.6	5.6	8.9
		Background	0.7 ± 0.2	1.1 ± 0.4	0.7 ± 0.3	0.6 ± 0.2	0.1 ± 0.1	0.3 ± 0.1

CERN/EP/PHYS 77-47

TABLE 3

	Predicted events	Experimentally found events		
		Raw data	Corrected	Excess
			Neutrino film	
e^- + lepton candidate	64.9 ± 6.3	55	68.0	3 ± 12
e^+, lepton candidate	4.6 ± 1.5	17	19.9	15 ± 5
e^- + hadrons	126.1 ± 13.9	88	114.5	-12 ± 20
e^+ + hadrons	3.5 ± 0.4	4	5.3	2 ± 3
Total e^- events	191.0 ± 21.3	143	182.5	-9 ± 28
Total e^+ events	8.1 ± 2.3	21	25.2	17 ± 6
			Antineutrino film	
e^- + lepton candidate	18.9 ± 2.1	15	19.7	1 ± 6
e^+ + lepton candidate	21.2 ± 1.1	17	20.5	-1 ± 5
e^- + hadrons	29.9 ± 4.3	34	41.2	11 ± 9
e^+ + hadrons	55.2 ± 7.1	45	59.2	4 ± 12
Total e^- events	48.8 ± 7.4	48	60.9	12 ± 12
Total e^+ events	76.3 ± 10.0	61	79.7	3 ± 15

FIGURE CAPTIONS

Fig. 1 Predicted neutrino and antineutrino spectra.

Fig. 2 Neutrino and antineutrino cross sections as a function of energy.

Fig. 3 Average square of the four-momentum transfer as a function of energy.

Fig. 4 Comparison of the y distributions for electron neutrino and antineutrino events with those for muon neutrino and antineutrino.

Fig. 5 Limits of M for various mixing parameters in neutrino and antineutrino oscillations. The 68% and 95% confidence level allowed regions are below the corresponding lines.

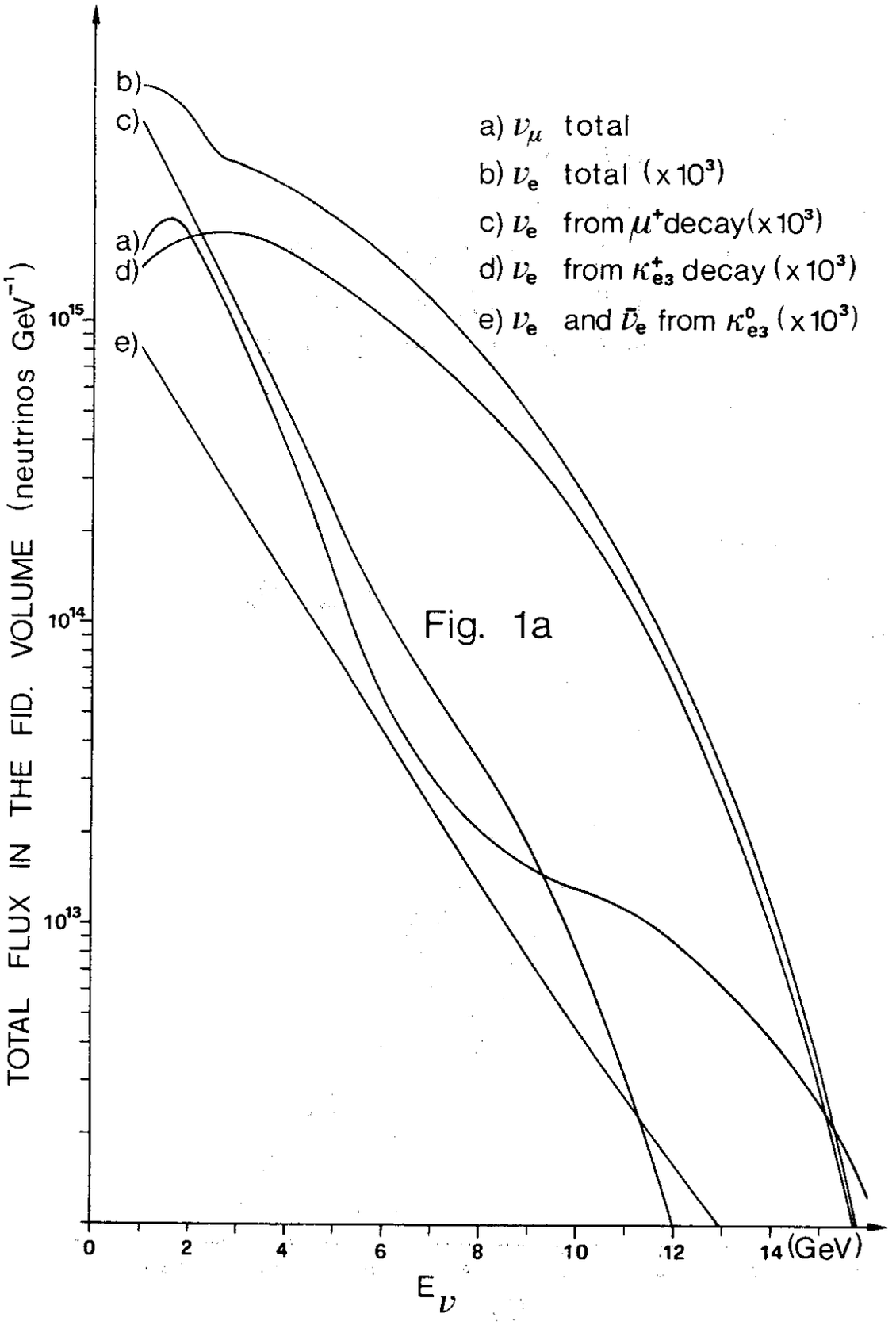
a) ν_μ total
b) ν_e total (x10³)
c) ν_e from μ^+decay(x10³)
d) ν_e from κ^+_{e3} decay (x10³)
e) ν_e and $\bar{\nu}_e$ from κ^0_{e3} (x10³)
TOTAL FLUX IN THE FID. VOLUME (neutrinos GeV⁻¹)
10¹⁵
10¹⁴
10¹³
0
2
4
6
8
10
12
14 (GeV)
E_ν

Fig. 1a

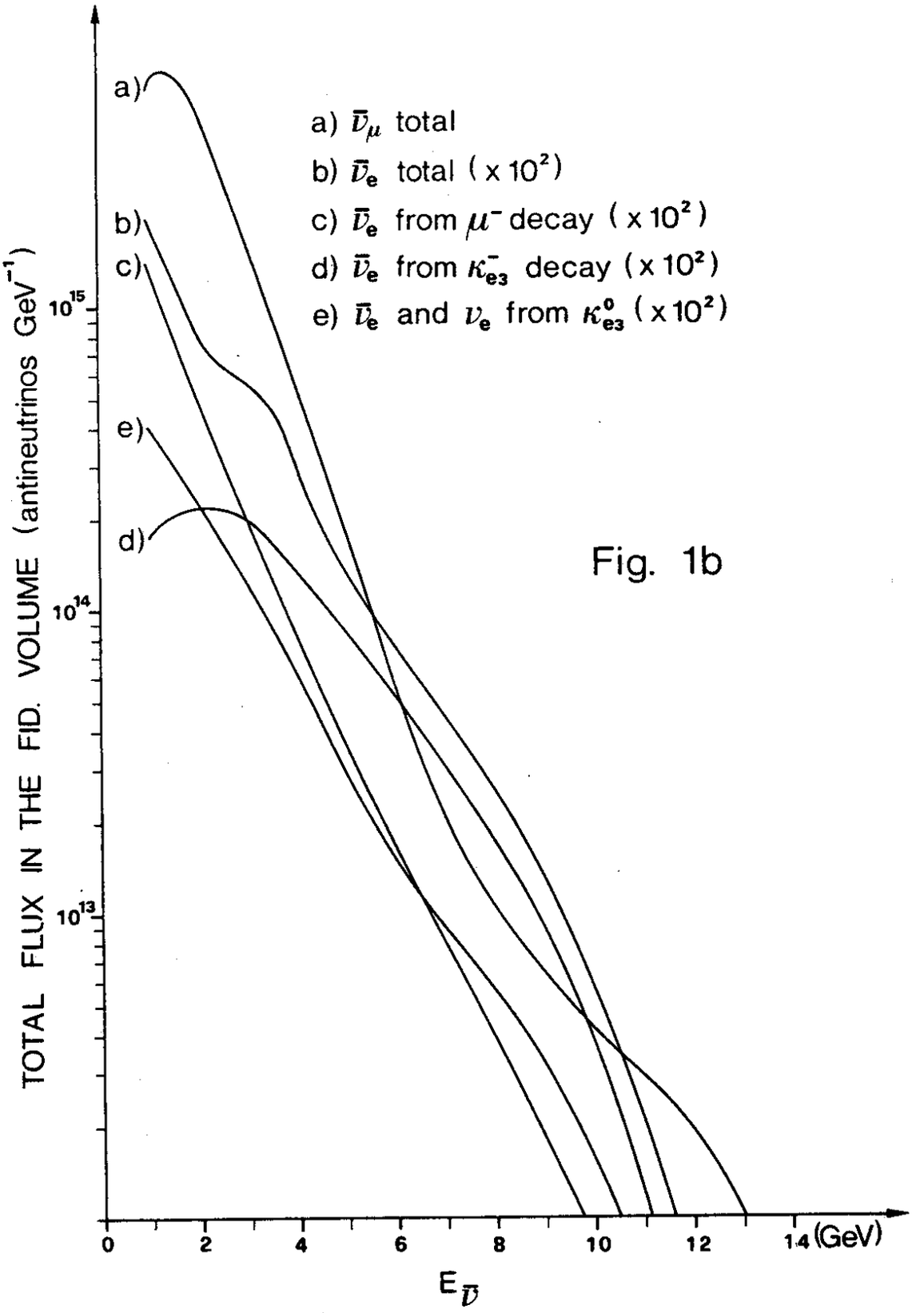
a) $\bar{\nu}_\mu$ total
b) $\bar{\nu}_e$ total (x 10^2)
c) $\bar{\nu}_e$ from μ^- decay (x 10^2)
d) $\bar{\nu}_e$ from κ^-_{e3} decay (x 10^2)
e) $\bar{\nu}_e$ and ν_e from κ^0_{e3} (x 10^2)
TOTAL FLUX IN THE FID. VOLUME (antineutrinos GeV^{-1})
10^{15}
10^{14}
10^{13}
0
2
4
6
8
10
12
14 (GeV)
$E_{\bar{\nu}}$

Fig. 1b

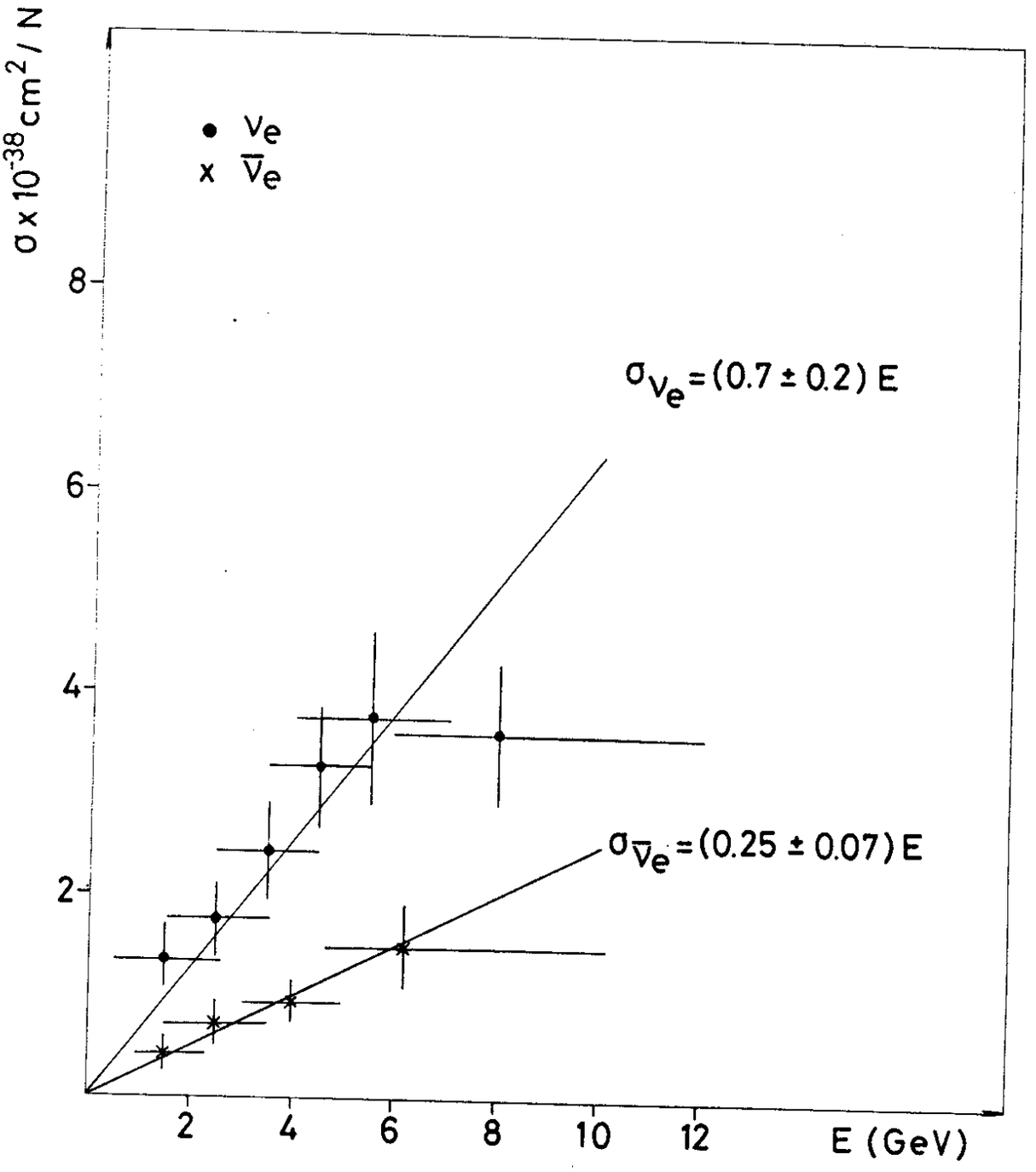

Fig. 2

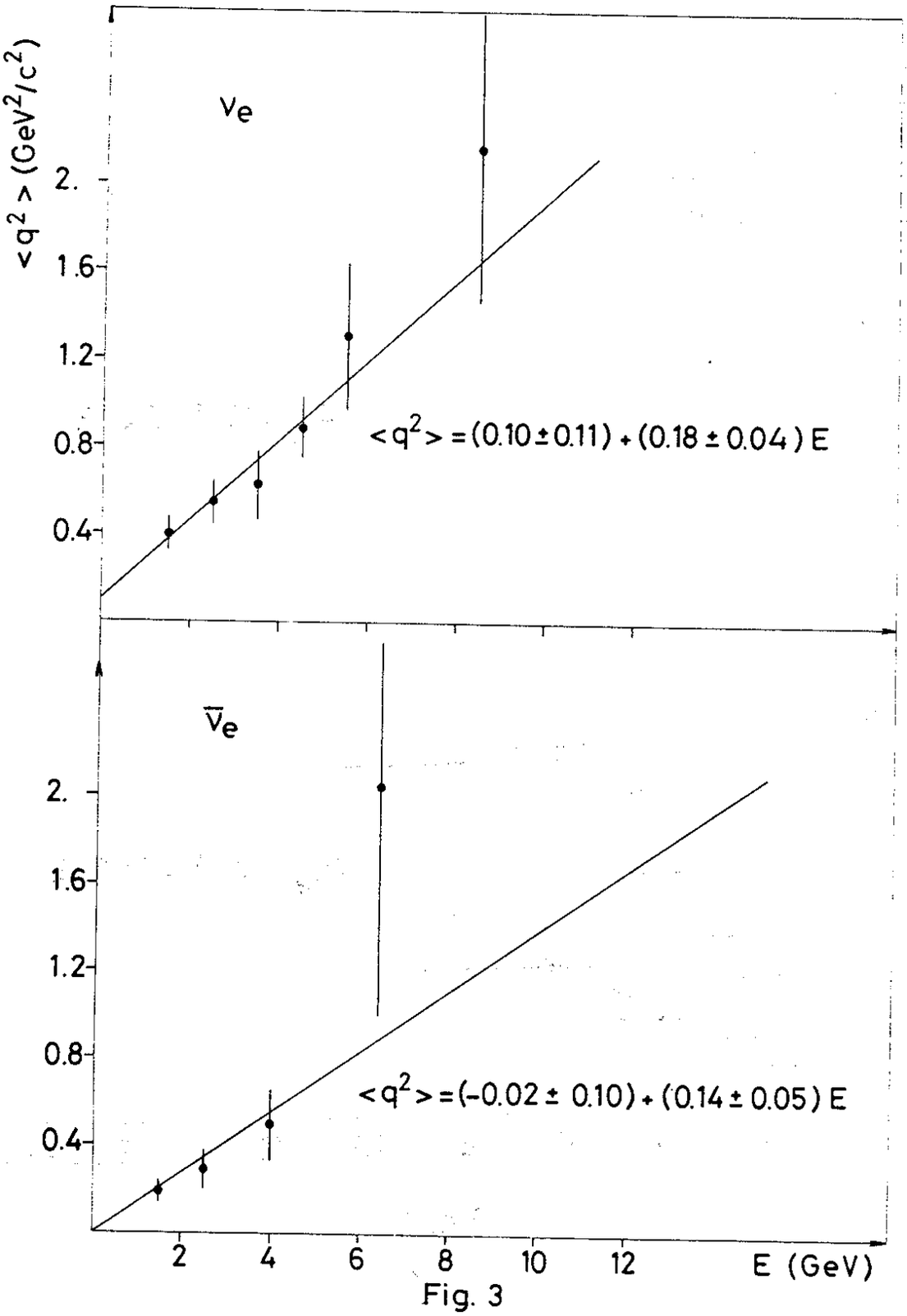
ν_e
$\langle q^2 \rangle$ (GeV^2/c^2)
2.
1.6
1.2
0.8
0.4
$\langle q^2 \rangle = (0.10 \pm 0.11) + (0.18 \pm 0.04)\,E$
$\bar{\nu}_e$
2.
1.6
1.2
0.8
0.4
$\langle q^2 \rangle = (-0.02 \pm 0.10) + (0.14 \pm 0.05)\,E$
2
4
6
8
10
12
E (GeV)

Fig. 3

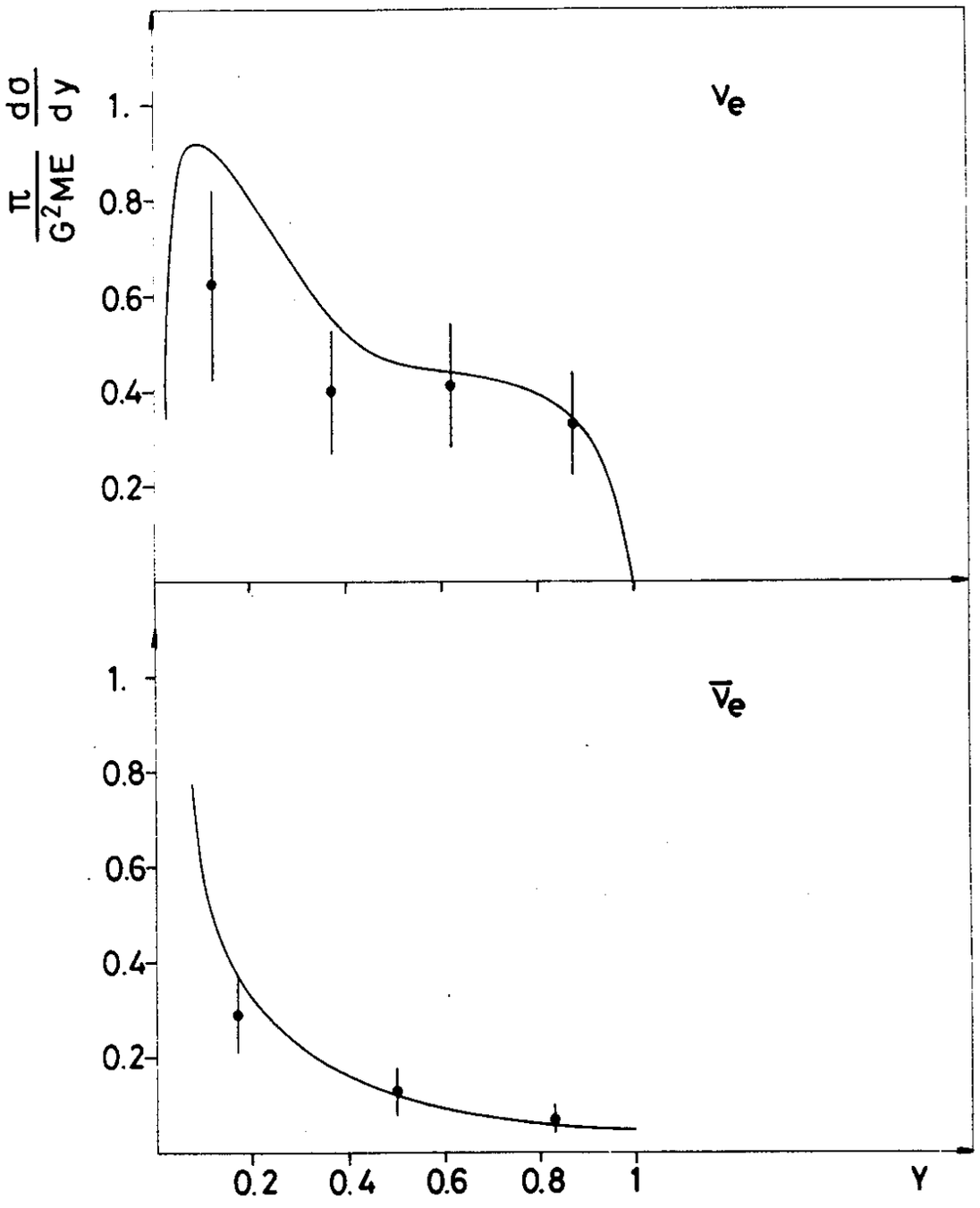
$\frac{\pi}{G^2ME}\frac{d\sigma}{dy}$
1.
0.8
0.6
0.4
0.2
ν_e
1.
0.8
0.6
0.4
0.2
$\bar{\nu}_e$
0.2
0.4
0.6
0.8
1
Y

Fig. 4

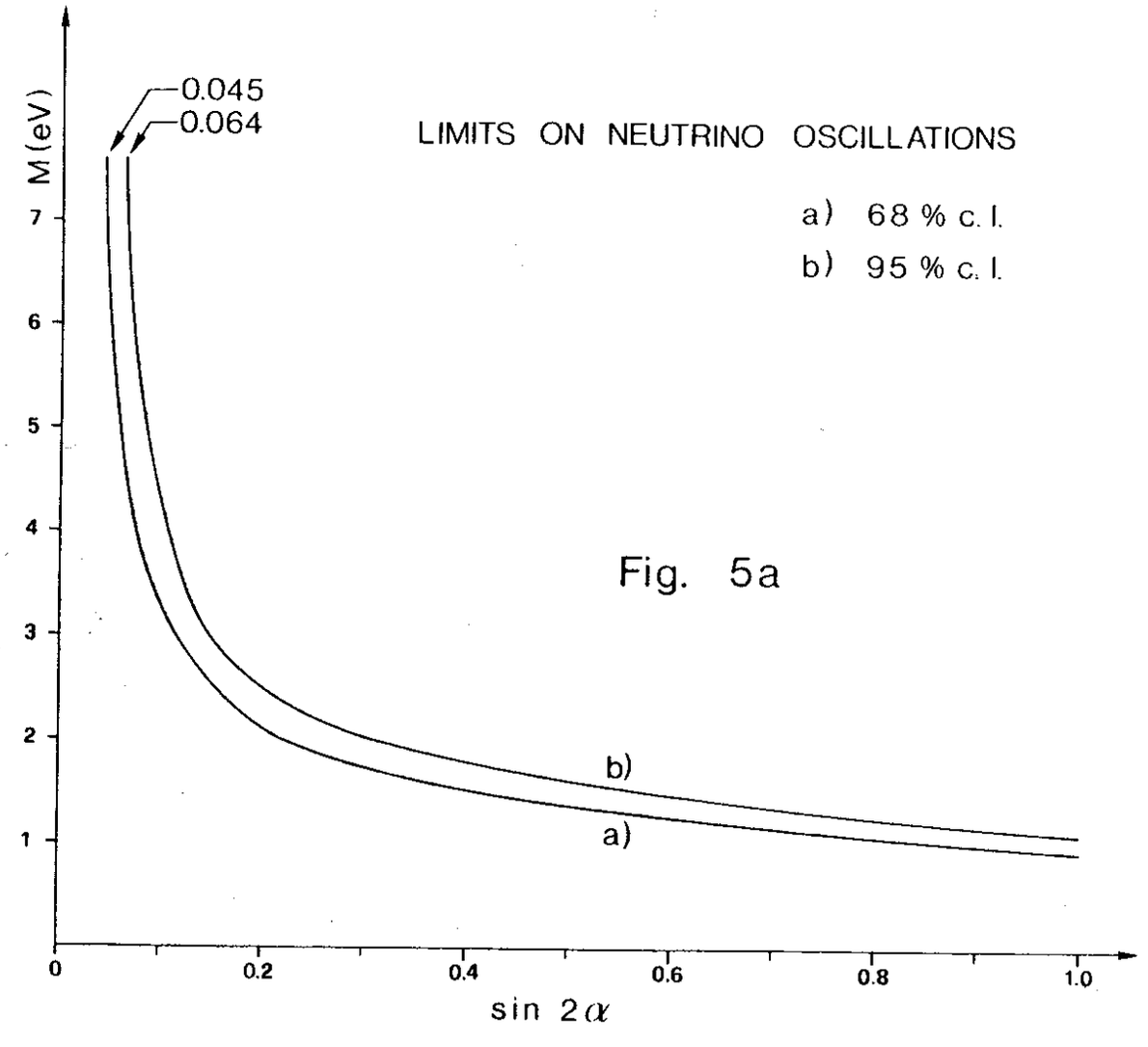
0.045
0.064
LIMITS ON NEUTRINO OSCILLATIONS
a) 68 % c. l.
b) 95 % c. l.
M (eV)
7
6
5
4
3
2
1
b)
a)
0
0.2
0.4
0.6
0.8
1.0
sin 2α

Fig. 5a

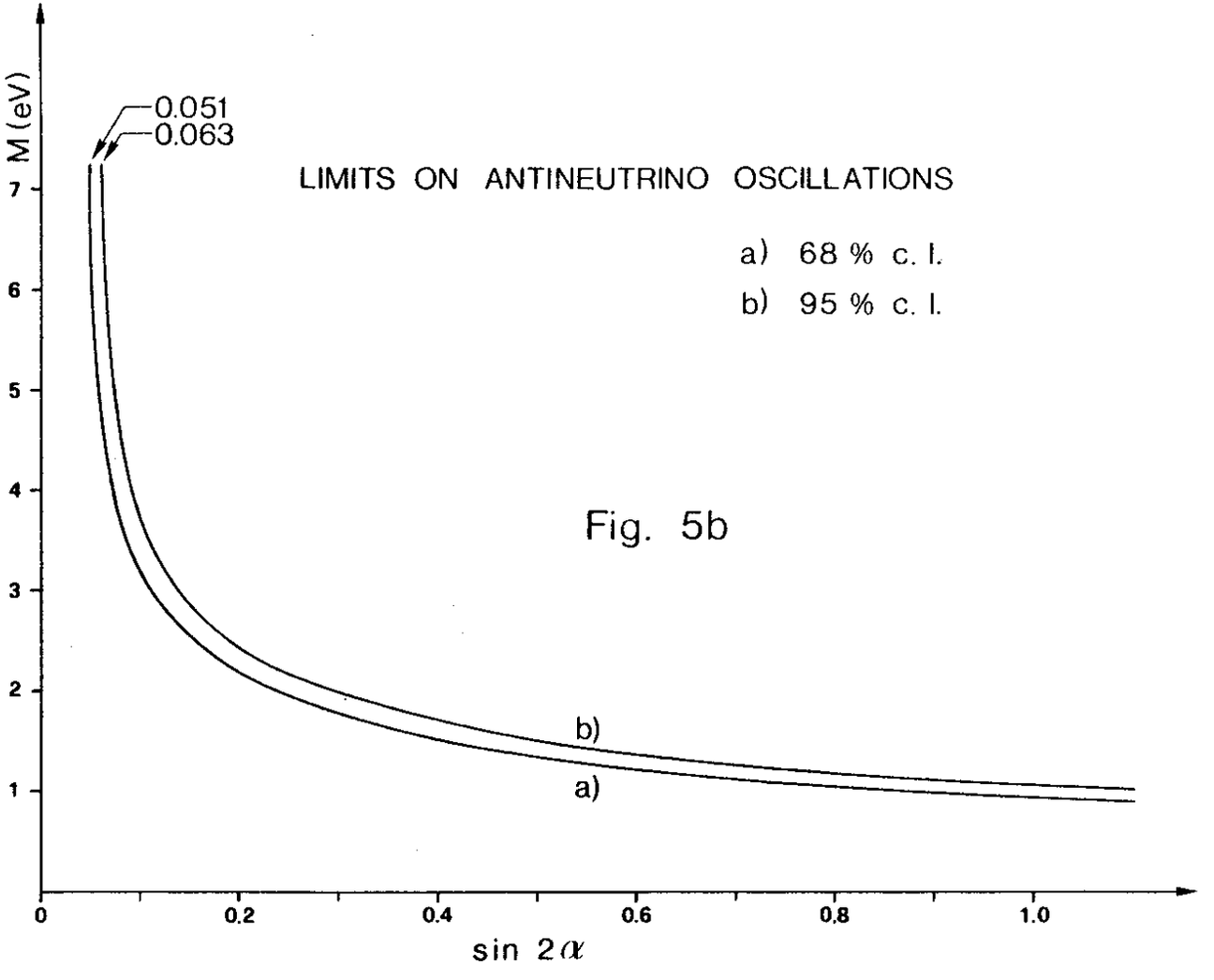
M (eV)
0.051
0.063
LIMITS ON ANTINEUTRINO OSCILLATIONS
a) 68 % c. l.
b) 95 % c. l.
b)
a)
sin 2α

Fig. 5b